

Star formation properties of UV selected galaxies in the ELAIS field

J. Iglesias-Páramo¹, V. Buat², J. Hernández-Fernández¹, C. K. Xu³,
D. Burgarella² and GALEX & SWIRE teams

¹Instituto de Astrofísica de Andalucía (C.S.I.C.), SPAIN
emails: jiglesia,jonatan@iaa.es

²Observatoire Astronomique de Marseille Provence, FRANCE
emails: veronique.buat,denis.burgarella@oamp.fr

³California Institute of Technology, Pasadena, USA
email: cxu@ipac.caltech.edu

Abstract. Properties related to dust attenuation and star formation of an UV selected sample of intermediate redshift galaxies are presented in this work. We find hints of a decrease of the L_{IR}/L_{FUV} ratio with increasing redshift at low values of the total luminosity. Downsizing is observed at all redshifts, and the SSFR is found to increase with increasing redshift at all stellar masses.

Keywords. galaxies: evolution

1. Introduction

This work intends to study the star formation properties of an UV selected sample ($m_{NUV} \leq 22.5$ ABmag) of galaxies in the redshift range $0.2 \leq z \leq 0.7$, taken from the ELAIS-N1 and ELAIS-N2 fields. The multiwavelength data used in this work come from GALEX (NUV, 2310Å), Spitzer/IRAC (3.6, 4.5, 5.8, 8.0μm), Spitzer/MIPS (24μm, 70μm, 160μm) and INT2.5m (U, g', r', i', Z). Both IR and optical data, as well as photo- z for all the galaxies, come from the SWIRE group (Rowan-Robinson *et al.* 2005). A set of synthetic SEDs from the GRASIL code (Silva *et al.* 1998) was used to fit the data. For each galaxy, L_{FUV} (1510Å), L_{IR} (8–1000μm), M^* and SFR are derived from the synthetic SEDs by using the bayesian statistics.

2. L_{IR}/L_{FUV} vs. total luminosity

L_{bol} (defined as $L_{FUV} + L_{IR}$) is a good tracer of the total luminosity emitted by young stars. In addition, L_{IR}/L_{FUV} indicates the dust attenuation of star forming galaxies. It has already been already reported in the literature that more luminous galaxies tend to show also a higher dust attenuation (e.g. Wang & Heckman 1996).

Figure 1 (left) shows L_{IR}/L_{FUV} as a function of L_{bol} . A direct comparison between the different redshift bins is not possible because the observational limit ($m_{NUV} \leq 22.5$ ABmag) translates to different luminosity limits. Therefore, we compare the samples at different redshift bins by performing a K-S test within regions (a) and (b). As indicated in Table 1, for region (a) the probabilities that all the samples come from the same population are extremely low. This is confirmed by the fact that the average values of L_{IR}/L_{FUV} for these samples decrease with increasing redshift. For region (b) the populations are not significantly different to that with $z \in [0.2, 0.3]$. In addition, the average values of L_{IR}/L_{FUV} are almost constant with redshift. These results together suggest

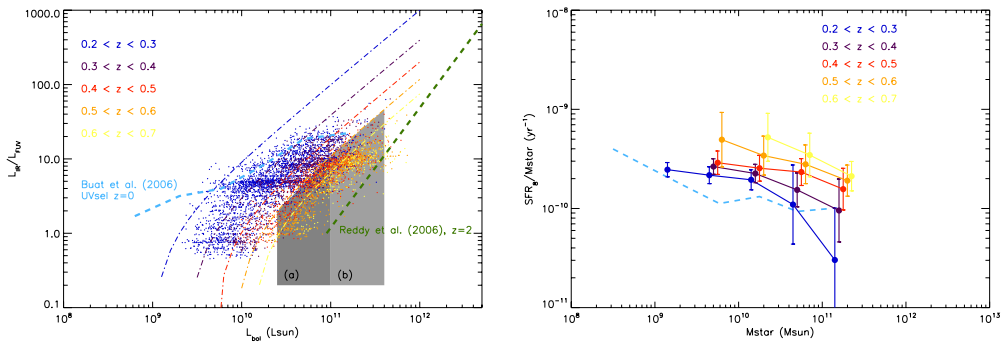


Figure 1. Left: $L_{\text{IR}}/L_{\text{FUV}}$ as a function of L_{bol} . Dot-dashed lines correspond to the observational limits above which no galaxies are allowed at each z . Bold dashed lines correspond to the relations of Buat *et al.* (2006, $z \approx 0$) and of Reddy *et al.* (2006, $z \approx 2$). The grey shaded regions are free of observational biases for galaxies with $z \in [0.2, 0.6]$. Right: Averaged SSFR as a function of M^* . The dashed line corresponds to the relation of Buat *et al.* (2006, $z \approx 0$).

Table 1. Results of the K-S test for the galaxies within regions (a) and (b) of Figure 1 (left).

Region	Pop. i	Pop. j	$N_{\text{gal},i}$	$N_{\text{gal},j}$	$P_{i,j}$
(a) $L_{\text{bol}} \in [2.5 \times 10^{10}, 10^{11}]$	$z \in [0.2, 0.3]$	$z \in [0.3, 0.4]$	139	127	0.38
	$z \in [0.2, 0.3]$	$z \in [0.4, 0.5]$	139	317	1.68×10^{-7}
	$z \in [0.2, 0.3]$	$z \in [0.5, 0.6]$	139	352	8.45×10^{-31}
(b) $L_{\text{bol}} \in [10^{11}, 4 \times 10^{11}]$	$z \in [0.2, 0.3]$	$z \in [0.3, 0.4]$	88	101	0.09
	$z \in [0.2, 0.3]$	$z \in [0.4, 0.5]$	88	309	0.55
	$z \in [0.2, 0.3]$	$z \in [0.5, 0.6]$	88	413	0.14

that the dust attenuation decreases with increasing redshift at low total luminosities, whereas this effect is not confirmed at high luminosities.

3. The specific SFR vs. stellar mass

Figure 1 (right) shows the SSFR as a function of the stellar mass. We find that at all redshifts less massive galaxies tend to show a larger SSFR, consistent with the downsizing picture already reported by several authors (e.g. Cowie *et al.* 1996; Brinchmann & Ellis 2000) for samples of galaxies selected on the basis of different wavelengths and at different redshifts. For a given stellar mass the average SSFR increases with redshift (a factor of $\simeq 8$ between $z = 0.25$ and 0.65 for $M^* \simeq 2 \times 10^{11} M_{\odot}$), which is consistent with an early epoch of star formation in massive galaxies (e.g. Feulner *et al.* 2005).

References

- Brinchmann, J., & Ellis, R. S. 2000, *ApJ*, 536, L77
- Buat, V., *et al.* 2006, *astro-ph/0609738*
- Cowie, L. L., Songaila, A., Hu, E. M., & Cohen, J. G. 1996, *AJ*, 112, 839
- Feulner, G., Gabasch, A., Salvato, M., Drory, N., Hopp, U., & Bender, R. 2005, *ApJ*, 633, L9
- Reddy, N. A., Steidel, C. C., Fadda, D., Yan, L., *et al.* 2006, *ApJ*, 644, 792
- Rowan-Robinson, M., *et al.* 2005, *AJ*, 129, 1183
- Silva, L., Granato, G. L., Bressan, A., & Danese, L. 1998, *ApJ*, 509, 103
- Wang, B., & Heckman, T. M. 1996, *ApJ*, 457, 645